

BBAMEM 74440

## A high-sensitivity differential scanning calorimetric study of the interaction of melittin with dipalmitoylphosphatidylcholine fused unilamellar vesicles

Thomas D. Bradrick<sup>1</sup>, Ernesto Freire<sup>2</sup> and S. Georgiou<sup>1</sup>

<sup>1</sup> Molecular Biophysics Laboratory, Department of Physics, University of Tennessee, Knoxville, TN  
and <sup>2</sup> Department of Biology, Johns Hopkins University, Baltimore, MD (U.S.A.)

(Received 1 December 1988)

**Key words:** Melittin; Protein-lipid interaction; Protein aggregation; Boundary lipid; DSC

High-sensitivity differential scanning calorimetry has been used to examine the interaction of bee venom melittin with dipalmitoylphosphatidylcholine fused unilamellar vesicles. Experiments were performed under conditions for which melittin in solution is either monomeric (in low salt) or tetrameric (in high salt). It was found that under both sets of conditions melittin abolishes the pretransition at a relatively high lipid-to-protein molar incubation ratio,  $R_i$  (about 200) and that at intermediate values of  $R_i$  it broadens the main transition profile and reduces the transition enthalpy. This provides evidence which suggests that melittin is at least partially inserted into the apolar region of the bilayer. Evident at low values of  $R_i$  are two peaks in the lipid thermal transition profiles, which may arise from a heterogeneous population of lipid vesicles formed through fusion induced by melittin, or by lipid phase separation. For those profiles which exhibited only one peak, transition enthalpies, normalized to those of the lipid in the absence of the protein, are plotted vs. the bound protein-to-lipid molar ratios for the experiments performed under the conditions which give monomeric and tetrameric melittin in solution. These plots yield straight lines, the slopes of which give the number of lipid molecules each protein molecule excludes from participating in the phase transition. These were found to be  $9.9 \pm 0.7$  and  $4.1 \pm 0.5$  for monomeric and tetrameric melittin, respectively. The results are discussed in terms of possible models for the binding of melittin to phospholipid vesicles. For simple hexagonal packing of lipid molecules, incorporation as an aggregate is favored when melittin is tetrameric in solution, whereas incorporation as a monomer is favored when melittin is monomeric in solution. For low-salt solutions, evidence is obtained for the contribution of free melittin to lipid fusion, perhaps by the formation of protein bridges between apposed vesicles.

### Introduction

Melittin is a small peptide of 26 amino-acid residues that constitutes approx. 50% of the dry weight of bee venom [1]. A considerable amount of work, using a number of different experimental techniques (e.g., steady-state and time-resolved fluorometry [2-7], NMR [8-11], ESR [12,13] and CD [8,14-16]), has been performed in an attempt to elucidate the effects which this protein has on phospholipid membranes. Of interest are the conformation and state of aggregation of the protein

in membranes, as well as the effect that the protein has on the properties of the lipid acyl chains. Such information is essential for achieving an understanding of the activity of the protein as a natural toxin and may also be useful for gaining insights into structures and processes (such as signal peptides, membrane proteins, membrane fusion and pore formation) which are of more general biological importance.

Differential scanning calorimetry is a powerful technique that allows the direct measurement of the thermodynamic properties of lipid vesicles. Such measurements can reveal the existence of distinct subpopulations within the lipid sample and the extent to which bound proteins affect its thermodynamic behavior. In the present study, we report the results of our systematic investigation of the effects of melittin on fused unilamellar vesicles of the zwitterionic phospholipid, DPPC, for a number of different lipid-to-protein molar ratios, made using high-sensitivity differential scanning calorimetry. Mea-

Abbreviations: DPPC, dipalmitoylphosphatidylcholine; FUVs, fused unilamellar vesicles;  $R_i$ , lipid-to-melittin molar incubation ratio;  $T_m$ , lipid-phase transition temperature.

Correspondence: S. Georgiou, Molecular Biophysics Laboratory, Department of Physics, University of Tennessee, Knoxville, TN 37996-1200, U.S.A.

measurements have been made under conditions for which the protein is monomeric or tetrameric in solution in order to explore the effect of protein aggregation on the lipid thermotropism. The results of the present study shed light on the state of aggregation of membrane-bound melittin, a subject which is currently under debate [11,17–19]. They also show that the protein exhibits a much greater affinity for the vesicles when it is tetrameric in solution. Furthermore, for monomeric melittin in solution, the free protein appears to make a contribution to melittin-induced vesicle fusion, perhaps through the formation of protein bridges between apposed vesicles.

## Materials and Methods

DPPC was obtained from Avanti Polar Lipids (Birmingham, AL), while melittin was obtained from ICN (Cleveland, OH). Both were used without further purification. Buffers used were 50 mM Tris/10 mM EDTA (pH 7) or 50 mM Tris/10 mM EDTA/2 M NaCl (pH 7) as noted. For the melittin concentrations used in these experiments, EDTA at a concentration of 10 mM is sufficient to eliminate the activity of any residual phospholipase A<sub>2</sub> in the sample (Ref. 20 and Bradrick and Georgiou, unpublished observations). All buffers were prepared from triply distilled water.

Lipid concentrations of the scanned samples were determined by a modified Bartlett phosphate assay as described by Mannetti [21]. Typically, the lipid concentration was about 2 mM. For each value of  $R$ , an individual sample was prepared by adding melittin to vesicles in a precisely measured volume from a 2 mM stock solution of the protein dissolved in the same buffer as was used to make up the lipid sample (i.e., low or high salt as noted). For the lowest ratio used ( $R$  = 20), the concentration of melittin (0.1 mM) was low enough for the protein to be in the monomeric form in the absence of salt [3]. After the addition of melittin, the protein/lipid samples were incubated for 30 min at 51°C in order to allow for binding of the protein to the lipid vesicles and their subsequent morphological changes.

The vesicle preparations used in these experiments were FUVs, which were prepared essentially as described by Schullery et al. [22]. DPPC dissolved in chloroform was dried under nitrogen and vacuum desiccated for 24 h to remove any remaining solvent. The dried lipid was then hydrated above  $T_m$  with 50 mM Tris/10 mM EDTA (pH 7) buffer and vortexed to give a dispersion with a concentration of 50 mg/ml. The dispersion was then sonicated to clearness in a Laboratory Supplies bath sonicator and centrifuged at 15000  $\times g$  for 60 min above the transition temperature to remove any remaining multilamellar vesicles. The sonicated vesicles were subsequently incubated at 4°C for 1

week before use. This low-temperature incubation induces the vesicles to fuse and produces a homogeneous population of single lamellar vesicles with a diameter of approx. 900 Å [23].

To obtain FUVs in a high-salt buffer the vesicles were prepared as just described. In addition, after the 1 week incubation at 4°C, a 5 ml solution of 10 mg/ml FUVs was dialyzed overnight at 55°C against 4 l of 50 mM Tris/10 mM EDTA/2 M NaCl (pH 7) buffer. For individual scans, aliquots of this lipid stock were diluted to the desired concentration.

Calorimetric measurements were performed with a Microcal MC1 or Microcal MC2 differential scanning calorimeter. The sensitivity and precision of the MC1 calorimetric unit were improved by the use of two separate Keithley amplifiers connected to the heat capacity and temperature outputs of the instrument. Each calorimeter was interfaced to an IBM PC through a Data Translation DT-805 A/D converter for automatic data collection and processing. Data were collected at 0.05°C intervals and stored for subsequent analysis. All the calorimetric scans were performed at a scanning rate of 20°C/h.

The fraction of melittin bound to FUVs was determined using two different methods. This information was necessary in order to obtain from  $R$ , the molar ratio of bound melittin to lipid. Samples having various values of  $R$  were prepared as described above. In the first method, they were then centrifuged at  $T_m$  for 0.5 h at 65000  $\times g$ . Following this, the sample tubes were removed and maintained at  $T_m$  while the aqueous portions were extracted. For samples prepared in low-salt buffer, the aqueous portion corresponds to the supernatant, which was quite easily drawn off. For samples prepared in high-salt buffer, the vesicles float and form a film on the surface of the solution. In order to avoid disturbing the film, portions of the aqueous phase were removed by piercing the side of the centrifuge tube with a hypodermic needle and drawing off the sample with a syringe. The concentration of melittin in the aqueous phase was determined by measuring the fluorescence intensity of the sample at 350 nm, with excitation at 280 nm. The excitation and emission bandwidths were both 10 nm. This was compared with the fluorescence intensity of an aqueous solution of known melittin concentration to determine the unknown concentration. The unknown samples were diluted as necessary in order to adjust their absorbances so as to maintain proportionality between fluorescence intensity and concentration. The aqueous portions were also assayed for phosphate, as described above, to determine how much lipid there was in them. Given the total amounts of lipid and melittin in the samples, as well as the lipid and melittin in the aqueous portions, we calculated the lipid-to-protein molar ratios of the pellets. In doing this, we took into account the fact that the absolute fluo-

rescence intensities of free and bound melittin differ at 350 nm. We assumed that the molar ratio in the pellet was also the ratio of melittin bound to the lipid in the supernatant and calculated the amount of free melittin based on this. In no case did the fraction of bound melittin differ from the uncorrected value (based simply on the total amount of melittin in the supernatant) by more than 10%.

In the second method, we determined the fraction of bound melittin by measuring at the lipid  $T_m$  the fluorescence anisotropy of melittin in lipid samples prepared as described above. The anisotropy,  $r$ , is given by

$$r = \frac{I_{VV} - I_{VH}(I_{HV}/I_{HH})}{I_{VV} + 2I_{VH}(I_{HV}/I_{HH})} \quad (1)$$

where V and H stand for vertical and horizontal orientation, respectively, and the first subscript refers to the excitation polarizer, while the second subscript refers to the emission polarizer. For a system consisting of free and bound ligand, the anisotropy of the sample is easily shown to be given by

$$r = \frac{\epsilon_f c_f q_f r_f + \epsilon_b c_b q_b r_b}{\epsilon_f c_f q_f + \epsilon_b c_b q_b} \quad (2)$$

where  $r$ ,  $q$ ,  $\epsilon$  and  $c$  are the emission anisotropy, fluorescence quantum yield, molar absorption coefficient and molar concentration of the ligand in the sample, subscripts b and f refer to bound and free ligand, respectively. Also, the fraction of bound ligand,  $f_b$ , is given by

$$f_b = c_b / c_t \quad (3)$$

where  $c_t = c_b + c_f$ . It follows from Eqns. 2 and 3 that

$$f_b = \frac{(\epsilon_f / \epsilon_b)(r - r_f)}{(q_b / q_f)(r_b - r) + (\epsilon_f / \epsilon_b)(r - r_f)} \quad (4)$$

Samples were excited at 297 nm in order to maximize the fluorescence anisotropy of melittin. Emission was observed at 335 nm. A bandwidth of 10 nm was used for both the excitation and emission monochromators.

We found the value of  $r_f$  in low-salt solution to be 0.049. We obtained a value for  $r_b$  in low-salt solution in the following way. First, we measured  $r$  for  $R_1 = 200$ , at which melittin is 95% bound as judged from our centrifugation data (see Results). We then used Eqn. 4 to calculate a value of 0.190 for  $r_b$ . It was necessary to obtain  $r_b$  in this way because, even at  $R_1 = 1000$ , melittin is not completely bound as calculated using our binding data. Thus, it was difficult to obtain a sample which contained completely bound melittin and which had a measurable fluorescence intensity. The alternative, which would have been to use a much higher concentration of melittin, would have required the use

of a much higher lipid concentration, for which there would have been a concomitant large increase in the amount of scattered light. For this reason it was also difficult to determine  $\epsilon_b$ , so that we took  $\epsilon_b$  to be approximately equal to  $\epsilon_f$ , as was previously established for small unilamellar vesicles [5].

We determined the value of  $q_b/q_f$  to be 1.74 for low-salt solutions. The fluorescence spectrum for bound melittin was corrected for scattered light as was previously described [5]. A lipid/protein sample with an incubation ratio of  $R_1 = 200$  was used to determine the bound spectrum. The quantum yield so obtained was corrected for the fraction of melittin that was actually free in solution (see above).

For high-salt solutions, we obtained values of 0.087, 0.141, and 1.70 for  $r_f$ ,  $r_b$  and  $q_b/q_f$ , respectively. A lipid/protein sample with an incubation ratio of  $R_1 = 200$  was used to obtain  $r_b$  and  $q_b$  here, as well. We note, however, that in high-salt solutions, melittin is completely bound at this ratio (see Results) so that, unlike the case of the low-salt solutions, no correction had to be made for partial binding.

When determining the contribution of lipid scattering to the polarized fluorescence signal, a correction was applied for the reduction in the turbidity of FUVs induced by melittin. (Such a reduction was previously reported for multilamellar vesicles [20].) This correction was determined by comparing the intensities of light scattered by the melittin/lipid sample and by a lipid-only solution at 540 nm, at which wavelength melittin does not fluoresce.

All fluorometric measurements were made on a spectrofluorometer, previously described [24]. All absorption measurements were made on a Varian Cary 2200 spectrophotometer.

## Results

Results from our measurements of the specific heats,  $C_p$ , for heating scans of DPPC FUVs incubated with melittin at various values for  $R_1$ , are shown in Figs. 1 and 2. Fig. 1 depicts  $C_p$  as a function of temperature for experiments performed in a low-salt buffer, while Fig. 2 shows the same for experiments performed in the presence of 2 M NaCl. The first panel (A) in each figure shows the transition profile for vesicles in the absence of melittin. In the case of a low-salt solution (Fig. 1), the value of the transition enthalpy was found to be 8.3 kcal/mol. This is in excellent agreement with the previously reported value of 8.4 kcal/mol for this quantity [25]. Moving through the figure from left to right, one can see from the next panel (B) that for  $R_1 = 193$  the lipid pretransition has been abolished and the maximum specific heat and the enthalpy have been reduced. An approximate doubling of the amount of melittin ( $R_1 = 107$ , panel C) causes a further reduction in the

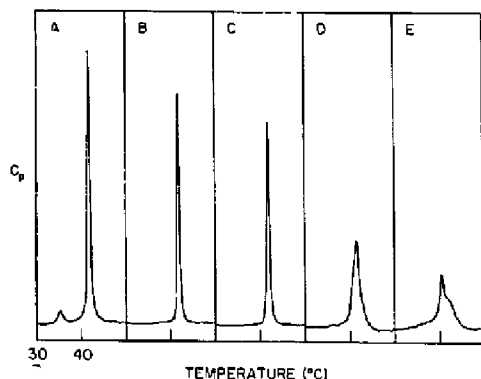


Fig 1 Plots of the specific heat,  $C_p$  (for heating scans) as a function of temperature for DPPC FUVs incubated with melittin at the following lipid-to-protein molar ratios  $R$ , in low-salt buffer (A) 0 (B) 193 (C) 107, (D) 33 and (E) 20. The temperature scale for each panel extends from 30 to 50°C. All of the profiles have the same vertical scale. Measurements were made on a Microcal MC1 high-sensitivity differential scanning calorimeter, the data were collected at 0.05°C intervals by an IBM PC equipped with a Data Translation DT-805 A/D converter. The scanning rate was 20°C/h. The buffer was 50 mM Tris/10 mM EDTA (pH 7) prepared in triply distilled water.

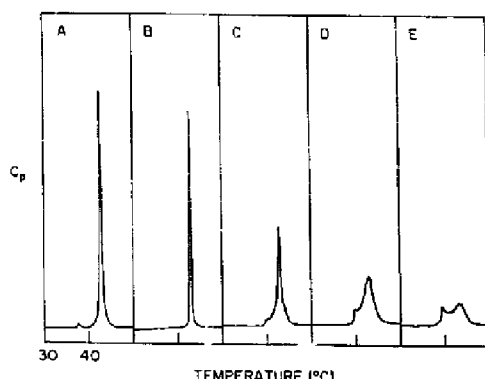


Fig 2 Plots of the specific heat,  $C_p$  (for heating scans) as a function of temperature for DPPC FUVs incubated with melittin at the following lipid-to-protein molar ratios  $R$ , in high-salt buffer (A) 0 (B) 162 (C) 46, (D) 24 and (E) 20. The temperature scale for each panel extends from 30 to 50°C. All of the profiles have the same vertical scale. Measurements were made on a Microcal MC2 high-sensitivity differential scanning calorimeter, the data were collected at 0.05°C intervals by an IBM PC equipped with a Data Translation DT-805 A/D converter. The scanning rate was 20°C/h. The buffer was 50 mM Tris/10 mM EDTA/2 M NaCl (pH 7) prepared in triply distilled water.

specific heat and enthalpy. The transition profile is still clearly symmetrical, however. The fourth panel (panel D,  $R_1 = 33$ ) continues the trend in the reduction in specific heat with increasing melittin concentration. There is also a concomitant reduction in the cooperativity of the transition, which is evidenced by the broadening of the transition profile. There has been little change in the transition enthalpy, however, between this ( $R_1 = 33$ ) and the previous incubation ratio ( $R_1 = 107$ ). (Indeed, they both possess approximately the same molar ratio of bound protein-to-lipid, see below.) Within experimental error, the transition temperature remains unchanged through panel D. One also observes the appearance of a shoulder on the low-temperature side of the peak. This shoulder seems to be centered at approx. 40.7°C (as judged from a larger-scaled plot of the profile, not shown) and has an area equal to about one-third that of the total profile area. The final panel (E) depicts the transition profile for  $R_1 = 20$ . The principal peak is now at 40.5°C and appears to correspond to the shoulder which was seen in the preceding profile (D). In fact, the height of this peak seems to have remained undiminished with the addition of more melittin and is located at the same (or a slightly lower) temperature. To the right of the new peak is what remains of the once principal peak, still centered at approx. 41.7°C, but which has been so reduced in cooperativity as to be spread out over a range of about 10°C.

Fig 2 shows the same type of progression for the case of protein and lipid in the presence of 2 M NaCl. As before, the first panel (A) gives the transition profile for the pure lipid in the absence of melittin. A value of 5.6 kcal/mol was obtained for the enthalpy of the transition under these conditions, as compared to 8.3 kcal/mol in the absence of salt. Also, the temperature corresponding to the peak was found to have increased slightly to 42.7°C, as was the temperature of the pretransition (from approx. 35°C in the case of low salt to approx. 37°C here). Clearly, the presence of salt at a high concentration has had an effect on the behavior of the lipid, which includes the dynamics of the acyl chains as well as interactions at the headgroups, with which the pretransition is associated. The next panel to the right (B) shows that the pretransition has been abolished by the time one reaches  $R_1 = 162$ . The addition of melittin has also reduced the height of the profile and the enthalpy of the transition. No effect is observed on the width of the transition, however. The middle profile (panel C,  $R_1 = 46$ ) continues the trend of the reduction of peak height and enthalpy with increasing melittin concentration. The peak has also become broader, which reflects a decrease in the cooperativity of the lipid phase transition. One also notes the appearance of a shoulder on the peak, centered at 40°C. This shoulder was first seen in profiles for molar ratios of  $R_1 = 65$  (data not shown). For  $R_1 = 24$  (panel D) the peak height has again been reduced and the profile has become much

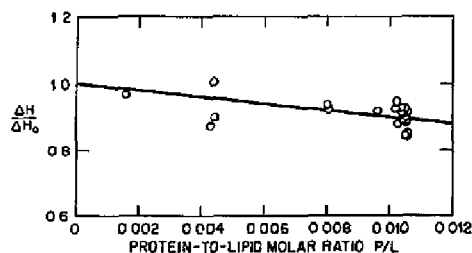


Fig. 3 Plot of the transition enthalpy  $\Delta H$  vs bound protein-to-lipid molar ratio  $P/L$  for DPPC FUVs incubated with melittin at various lipid-to-protein molar ratios. The buffer was 50 mM Tris/10 mM EDTA (pH 7) prepared in triply distilled water. The enthalpies have been normalized to that of the vesicles in the absence of protein,  $\Delta H_0 = 8.3$  kcal/mol. The straight line represents the best fit to the data for a  $y$ -intercept equal to unity. The slope, which gives the number of boundary lipid molecules per protein molecule, was determined to be  $9.9 \pm 0.7$ . Protein/lipid samples for which the profiles exhibited more than a single peak ( $R_1 \leq 30$ ) were excluded from this graph.

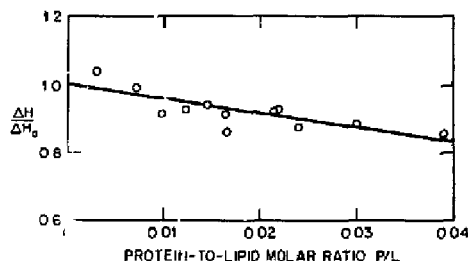


Fig. 4 Plot of the transition enthalpy  $\Delta H$  vs bound protein-to-lipid molar ratio  $P/L$  for DPPC FUVs incubated with melittin at various lipid-to-protein molar ratios. The buffer was 50 mM Tris/10 mM EDTA/2 M NaCl (pH 7) prepared in triply distilled water. The enthalpies have been normalized to that of the vesicles in the absence of protein,  $\Delta H_0 = 6.6$  kcal/mol. The straight line represents the best fit to the data for a  $y$ -intercept equal to unity. The slope, which gives the number of boundary lipid molecules per protein molecule, was determined to be  $4.1 \pm 0.5$ . Protein/lipid samples for which the profiles exhibited more than a single peak ( $R_1 \leq 40$ ) were excluded from this graph.

broader. Finally, the above characteristics are further accentuated in the last profile (panel E,  $R_1 = 20$ ). In fact, the degree of change from the previous profile is quite pronounced considering the small change in the incubation ratio (from  $R_1 = 24$  to  $R_1 = 20$ ), the principal (i.e., original) peak has been greatly reduced in height (although not significantly broadened), while the peak on the low-temperature side has increased its contribution to the overall profile. Interestingly, the high-temperature peak was shifted to  $43.5^\circ\text{C}$ , which amounts to an increase of almost  $1^\circ\text{C}$  relative to the transition temperature of the free lipid in high salt.

In order to determine whether the calorimetric scans were reversible, we also performed cooling scans followed by heating scans on the same samples, for a wide range of values for  $R_1$  in low- and high-salt solutions (profiles not shown). We found that in the case of the high-salt samples, the calorimetric scans were reversible for the whole range of incubation ratios  $R_1$  used in our study. The scans were also reversible for low-salt samples and  $R_1 \geq 30$ . In the case of the low-salt samples for  $R_1 \leq 30$ , heating scans always gave a simpler, less structured transition profile than did the cooling scans (The latter showed a smaller peak on the low-temperature side of the main transition profile).

Figs. 3 and 4 show the transition enthalpies,  $\Delta H$ , normalized to the enthalpies of the free lipid,  $\Delta H_0$ , plotted vs the corresponding bound protein-to-lipid molar ratios,  $P/L$ , for the low- and high-salt experiments, respectively. The corresponding values for  $\Delta H_0$  were found to be 8.3 and 6.6 kcal/mol. In the case of Fig. 3, the results from the low-salt binding experiments were used to correct the molar incubation ratios  $R_1$  for

the presence of free protein in order to obtain the molar ratios of bound melittin to lipid. Fig. 5, which shows the percentage of bound melittin as a function of  $R_1$  for samples in low-salt solution, was used to carry out this correction\*. The clustering of points in Fig. 3 at a protein-to-lipid molar ratio of about 0.01 is due to the fact that, below an incubation ratio of  $R_1 = 100$ , the lipid vesicles rapidly approach being saturated with melittin to the minimum lipid-to-bound-protein molar ratio of 93. No correction of the incubation ratios was necessary in the case of Fig. 4, as in high-salt solutions we have found that melittin is completely bound over the range of values shown. As can be seen, the low- and high-salt data are fitted quite well by straight lines and can be modeled by the equation [28]

\* The solid line shown in Fig. 5, which is seen to fit the data quite well, was obtained from a Scatchard-plot analysis of the data. Values of  $K = (2.4 \pm 0.4) \cdot 10^6 \text{ M}^{-1}$  and  $n = 93 \pm 20$  were obtained for the binding constant and the number of lipids per melittin binding site, respectively. These values are of the same order of magnitude as those obtained for other melittin/lipid systems [16,26]. We note that at low lipid-to-protein molar incubation ratios,  $R_1$ , melittin forms nonvesicular structures [27] which presumably have a different affinity for melittin than do FUVs. Therefore, the binding cannot be assumed to be reversible and this description should be considered as being only phenomenological. The data were obtained from individual samples prepared with the desired values of  $R_1$  (as were the samples used in the calorimetric measurements), not from a single lipid sample that was titrated with melittin. Consequently, these considerations in no way affect the data analysis which yields the number of boundary lipids per protein or the presentation of the data in Fig. 3.

$$\frac{\Delta H}{\Delta H_0} = 1 - \langle n_i \rangle (P/L) \quad (5)$$

where  $\langle n_i \rangle$  is the average number of boundary lipid molecules per protein molecule and  $P/L$  is the molar ratio of bound protein to lipid. Least-squares fits to the data using this model gave values for the slope of  $9.9 \pm 0.7$  and  $4.1 \pm 0.5$  lipid molecules per protein molecule for low- and high-salt conditions, respectively. (Data for melittin-to-lipid ratios which exhibited two peaks in the transition profiles,  $R_1 \leq 30$  for low-salt and  $R_1 \leq 40$  for high-salt solutions, were excluded from Figs 3 and 4 and from these calculations.)

## Discussion

Previous work has shown that melittin exerts a strong perturbing influence on the order and dynamics of the lipid acyl chains [7,29,30]. Melittin has also been reported to possess fusogenic activity [31–34], the rate of which was recently shown to be strongly dependent on the state of aggregation of the protein in solution [33]. The effects of the protein are quite strong and seem to stem not only from the direct perturbing influence that it has on the lipid molecules in its immediate vicinity but also from its ability to induce large-scale structural reorganization of lipid vesicles.

In the present work we show that the addition of melittin at low values of  $R_1$  to FUVs composed of the zwitterionic phospholipid DPPC results in transition profiles which have two peaks. We note that FUVs of zwitterionic phospholipids have been reported to undergo fusion in the presence of melittin [31]. Also, multilamellar and small unilamellar vesicles of zwitterionic phospholipids have been shown through electron microscopy, light scattering and gel filtration [27] to form a heterogeneous population of vesicles and nonvesicular structures for values of  $R_1$  smaller than 30. In this heterogeneous distribution, new structures, formed through the fusogenic properties of the protein, were found to coexist with the remaining nonfused lipid vesicles. The existence of the distinct peaks seen for small values of  $R_1$  in the thermodynamic profiles presented here (Figs. 1 and 2) may be the result of melittin having induced only some of the vesicles to fuse and so produced a heterogeneous population of lipid vesicles which exhibit differing melting behaviors. An alternative explanation for the origin of this phenomenon is phase separation. In the vesicles used here, which were composed of a single type of lipid, this corresponds to the segregation of membrane-bound melittin into protein-rich domains in the bilayer, with the concomitant formation of protein-poor domains. The various domains with their different local lipid-to-protein ratios would presumably exhibit different lipid melting profiles. On the basis of these data we are not able to

choose between this hypothesis and that based on the formation of heterogeneous structures through fusion. We are attempting to address this issue through ongoing work in our laboratory. We note that two studies which included calorimetric measurements, obtained data for low lipid-to-melittin molar ratios and tetrameric melittin in solution which the authors have interpreted as exhibiting melittin-induced phase separation. Bernard et al. [4] for negatively charged dimyristoylphosphatidic acid multilamellar vesicles, and more recently, Batenburg et al. [26] for dielaidoylphosphatidylethanolamine multilamellar vesicles.

In comparing the fusogenic properties of melittin in the cases of low- and high-salt solutions, it is of interest to note that a recent study [33] has reported a much higher rate of fusion for the latter. This may indicate that the mechanisms of fusion are also different. For the high-salt solutions used in the present study, melittin is almost completely bound for values of  $R_1$  at least as low as 25 (the lowest ratio we have used here), whereas for low-salt solutions it is essentially bound for  $R_1$  values down to about 100 (100 is approximately the minimum molar ratio of lipid to bound protein, this can easily be deduced from the data presented in Fig. 5). Consequently, the evolution of the thermal transition profiles as  $R_1$  decreases for the former solutions (Fig. 2) stems exclusively from the effect of bound melittin, whereas for the latter solutions (Fig. 1) free melittin appears to make a contribution as well for  $R_1 \leq 100$ . If melittin which is free in solution plays a role in vesicle fusion, then this process presumably becomes more efficient as the amount of free melittin increases for values of  $R_1$  progressively lower than 100. This could explain why the low-salt profiles continue to evolve for  $R_1 \leq 100$ , even though the ratio of lipid to bound melittin remains virtually unchanged. A plausible mechanism for the enhancement of fusion by free melittin may be the formation of protein bridges between apposed vesicles. This could be accomplished by the anchoring of the positively charged N- and C-termini of the protein on the outer surfaces of the two bilayers. This type of mechanism (i.e., bridge formation) has been suggested to explain how the  $\text{Ca}^{2+}$ -induced fusion of charged vesicles is facilitated by the adrenal medullary protein synexin [35] and also how poly(L-lysine) causes the fusion of vesicles composed of dipalmitoylphosphatidylglycerol [36].

In preparing the lipid/melittin samples used in this study we have observed that for low values of  $R_1$  (less than about 30) the low-salt samples show a considerable increase in turbidity when they are allowed to warm above  $T_m$ . This suggests that for samples with  $R_1 \leq 30$  the discoidal and/or other nonvesicular structures formed through the fusogenic properties of melittin [27] may coalesce to form larger structures when the sample temperature is allowed to pass above  $T_m$ . Such a transi-

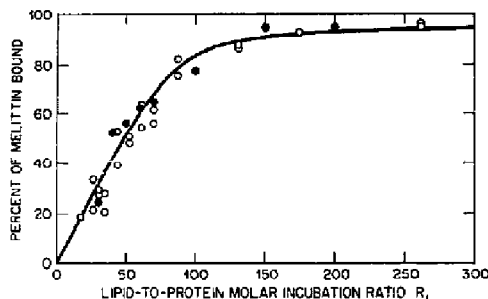


Fig. 5 Plot of the percent of total melittin added which is bound to DPPC FUVs in 50 mM Tris/10 mM EDTA (pH 7) buffer at 41°C, as a function of the lipid-to-protein molar incubation ratio  $R_i$ . Open circles denote values obtained using ultracentrifugation, whereas closed circles denote values obtained using fluorescence anisotropy (see Materials and Methods). These data were used with the molar incubation ratios  $R_i$  to obtain the molar ratio of bound melittin to lipid for the data presented in Fig. 3. Also shown is the best fit to the data (solid line) which was generated using the apparent values for the binding constant ( $K = 2.4 \cdot 10^6 \text{ M}^{-1}$ ) and the number of lipids per protein binding site (93) obtained via a computer analysis of the data (see first footnote). The data and curve are for a lipid concentration of 1 mM.

tion from nonvesicular to vesicular structures was previously observed for melittin incubated with DPPC multilamellar vesicles at low lipid-to-melittin molar ratios [37]. Our calorimetric measurements made on low-salt samples reveal that the transition profiles are reversible for  $R_i \geq 30$  and irreversible for  $R_i \leq 30$  (see Results). The nonvesicle-to-vesicle transition may be the source of this "irreversibility" for the latter ratios. It may be argued that the scanning rate used in these experiments (20°C/h) is too fast for this process, which is taking place in addition to the melting of the lipid acyl chains, to adequately approximate equilibrium thermodynamics. Scanning at 10°C/h, the slowest rate possible for the MC2 microcalorimeter, did not significantly change the melting behavior, however. Alternatively, the samples may be showing true irreversibility or hysteresis-like behavior, so that the types of structure one ends up with (in, for instance, passing through  $T_m$ ) may depend on those with which one started. Concerning this latter possibility, however, we observed that for repeated heating and cooling scans performed on the same sample, there was very little difference between scans having the same direction in temperature change.

For all values of  $R_i$ , irreversibility was not observed in the heating and cooling scans made on high-salt samples. This may be the result of the salt ions having stabilized the structures which were formed through melittin-induced fusion, so that upon passing through the lipid  $T_m$  they do not coalesce, unlike what we suggest may be the case for the low-salt samples with

small values of  $R_i$ . In this respect, we did not observe a significant change in the turbidity of high-salt samples with low values of  $R_i$  when they were cycled through the lipid transition temperature. This is in contrast to the behavior of the low-salt samples. An alternative explanation for the difference in reversibility seen between the low- and high-salt samples is that fusion as induced by tetrameric melittin may lead to structures that are inherently more stable than those that are formed through monomer-induced fusion. With regard to this latter hypothesis, monomeric and tetrameric melittin have been reported [33] to cause greatly different rates of vesicle fusion. This suggests that they may also have different fusion mechanisms, which may lead to different structures being formed in the two cases.

There has been considerable discussion concerning the conformation and state of aggregation of membrane-bound melittin. Several models for the former have been considered, including the wedge [38,39], the trans-membrane  $\alpha$ -helix [39] and an  $\alpha$ -helix with its axis parallel to the bilayer surface [40]. These models all assume that the protein exists as a monomer when bound to the membrane. Conflicting conclusions have been reached, however, concerning the state of aggregation of melittin in lipid vesicles [17–19]. These studies have used the technique of resonance energy transfer and have reported very different findings for melittin bound to dimyristoylphosphatidylcholine small unilamellar vesicles. Hermetter and Lakowicz [18] have concluded that bound melittin is monomeric in the presence and in the absence of 2 M NaCl, whereas Vogel and Jähnig [17] have concluded that it is tetrameric in the absence of 2 M NaCl. Talbot et al. [19] have found that the state of aggregation of membrane-bound melittin depends on the salt concentration. Low-salt solutions were found to have melittin bound as a monomer, while solutions which contain 0.5 M NaCl were found to have melittin bound as a monomer and mixed oligomers. Vogel and Jähnig [17] have also presented a model for the tetramer that consists of four bent  $\alpha$ -helices (the melittin monomers) which are approximately parallel with one another and which are oriented so that the hydrophilic amino-acid residues are on the inside of the tetramer (which may serve as a channel or pore [41,42]). The hydrophobic residues are on the outside and are exposed to the apolar interior of the bilayer into which the aggregate is embedded (see Fig. 10, Ref. 17). As was pointed out by Talbot et al. [19], the differing results of the three resonance energy transfer studies [17–19] regarding the state of aggregation of membrane-bound melittin may be due to differences in the types of protein modification made.

In addition to the above resonance energy transfer studies, Stanislawski and Rutergans [11] have used  $^{13}\text{C}$ -NMR to investigate the conformation and state of aggregation of membrane-bound melittin. They have

studied the binding of tetrameric melittin\* (labeled with two  $^{13}\text{C}$ -methyl groups each at lysine residues 7, 21 and 23) to dimyristoylphosphatidylcholine unilamellar vesicles. Under these conditions, they report that melittin binds as a monomer having the wedge conformation. Considering the disagreement that exists between the results of these studies [11,17–19], all of which used chemically modified melittin, it would be of great interest to obtain information about the state of aggregation of nonmodified melittin in lipid vesicles. The results of the present study provide such information which is discussed below.

The shape of the  $\alpha$ -helical monomer may be approximated by a cylinder which has a radius of 5 Å [43] and a length that would just span the bilayer [17]. Its cross-sectional area is thus almost identical to the headgroup area of DPPC above the transition temperature [44]. For hexagonal packing of the lipid molecules, one would therefore expect that for a melittin monomer which spans the bilayer each protein molecule would be surrounded by 12 lipid molecules (six in each leaflet of the bilayer). The protein would presumably prevent all 12 lipid molecules from participating in the phase transition, so that 12 would be the predicted number of boundary lipids in this case. In contrast to this, the model proposed by Vogel and Jähnig [17] for the membrane-bound tetramer suggests that the protein aggregate would be surrounded by approx. 20 lipid molecules (ten in each leaflet of the bilayer), or five lipid molecules per protein molecule. Our results show that for high-salt solutions in which melittin is tetrameric each bound protein molecule removes between four and five lipid molecules from participating in the phase transition. This finding is in good agreement with our prediction which is based on the tetramer model of Vogel and Jähnig. For other models of the membrane-bound monomer, melittin would still possess boundary lipids much greater in number than that which we have found for the high-salt solutions. For the wedge model, each half would seem to be in contact with six lipid molecules. Also, for a monomer only partially embedded into the bilayer, the hydrophobic segment would be surrounded by six lipids and, in addition, the segment bound to the membrane surface would perturb the lipid molecules beneath it. Thus, despite the different possible conformations for a membrane-bound monomer,

there is a significant difference between their predicted number of boundary lipids and that predicted by the tetramer model\*. The fact that our value for the number of boundary lipids is slightly lower than that predicted by the latter may be due to simplifying assumptions made about the sizes and packing of the lipid and protein molecules, and to the presence of some higher-order melittin oligomers which would serve to lower somewhat the measured number of boundary lipids per protein. A transmembrane melittin hexamer, for example, would possess 24 boundary lipids (12 in each leaflet of the bilayer), or four lipids per protein molecule. That our inference regarding the state of aggregation of lipid-bound melittin differs somewhat from that of Talbot et al. [19], who found monomers and mixed oligomers at a concentration of 0.5 M NaCl, may be due to differences in the salt concentration used. For the concentration of melittin used in Ref. 19, the protein is not completely tetrameric in solution at 0.5 M NaCl, whereas for the melittin and salt (2 M NaCl) concentrations used in the present study the protein is completely tetrameric in solution [3].

In contrast to the above, the results of our experiments in low-salt solutions where melittin is monomeric suggests that melittin binds to lipid vesicles as a monomer under these conditions. This is evidenced by the good agreement between our value for the number of boundary lipids per protein (ten) and the number predicted by the different models (approx. 12, depending on the degree of insertion of the protein into the bilayer).

#### Acknowledgements

This work was supported by Research Grants GM32433 (to S.G.) and GM37911 (to E.F.) from the National Institutes of Health. T.D.B. and S.G. would like to thank Dr. Panayiotis P. Constantinides, LipoGen Inc. for very helpful discussions.

#### References

- Habermann E (1980) in *Natural Toxins* (Eaker, D. and Wadström, T. eds.) pp. 173–181. Pergamon Press, New York.
- Mollay C and Kreil, G (1973) *Biochim. Biophys. Acta* 316, 196–203.
- Talbot, J.C., Dufourcq J., Desnoy J., Faucon J.-F. and Lussan, C. (1979) *FEBS Lett.* 102, 191–193.
- Bernard, E., Faucon J.-F. and Dufourcq J. (1982) *Biochim. Biophys. Acta* 688, 152–162.
- We note that Mollay [45] has obtained a value of  $8 \pm 3$  for the number of boundary lipids per protein for DPPC multilamellar vesicles and melittin that was tetrameric in solution. (This value was obtained from Fig. 2 of Ref. 45.) Our value for tetrameric melittin is close to the lower limit of this. This difference presumably arises from melittin having different degrees of interaction with the lipids of the various lamellae.

\* Unlike the present study and those of Refs. 17–19 these authors have obtained tetrameric melittin in solution by using a very high concentration of melittin in a low-salt solution. With respect to this difference, ionic effects may play a role in the binding of melittin to vesicles: by shielding charges on the lipid and on the protein. The high melittin concentrations needed to ensure a melittin tetramer in low-salt solution, however, would have necessitated our using extremely high lipid concentrations (up to about 500 mM). These pose serious technical difficulties that prevented the quantification of these effects in the present study.



- 5 Georghiou, S, Thompson, M and Mukhopadhyay, A K (1982) *Biochim Biophys Acta* 688, 441-452
- 6 Quay S C and Condie, C C (1983) *Biochemistry* 22, 695-700
- 7 Bradrick, T D, Dasseux, J-L, Abdalla, M, Amnzadeh, A and Georghiou, S (1987) *Biochim Biophys Acta* 900, 17-26
- 8 Strom, R, Crifo, C, Vitu, V, Guidoni, L and Podo, F (1978) *FEBS Lett* 96, 45-50
- 9 De Bonv J, Dufourcq, J and Clin, B (1979) *Biochim Biophys Acta* 552, 511-514
- 10 Brown, L R, Braun, W, Kumar, A and Wuthrich, K (1982) *Biophys J* 37, 319-378
- 11 Stanislawski, B and Ruterjans, H (1987) *Eur Biophys J* 15, 1-12
- 12 Williams, J C and Bell, R M (1972) *Biochim Biophys Acta* 288, 255-262
- 13 Hegner, D, Schummer, U and Schnepel, G H (1973) *Biochim Biophys Acta* 291, 15-22
- 14 Drake, A F and Hider, R C (1979) *Biochim Biophys Acta* 555, 371-373
- 15 Knöppel, E, Eisenberg, D and Wickner, W (1979) *Biochemistry* 18, 4177-4181
- 16 Vogel, H (1981) *FEBS Lett* 134, 37-42
- 17 Vogel, H and Jahng, F (1986) *Biophys J* 50, 573-582
- 18 Hermetier, A and Lakowicz, J R (1986) *J Biol Chem* 261, 8243-8248
- 19 Talbot, J C, Faucon, J F and Dufourcq, J (1987) *Eur Biophys J* 15, 147-147
- 20 Dasseux, J-L, Faucon, J-F, Laffleur, M, Pérolet, M and Dufourcq, J (1984) *Biochim Biophys Acta* 775, 37-50
- 21 Marin, G V (1962) *J Lipid Res* 3, 1-20
- 22 Schullery, S E, Schmidt, C F, Feigner, P, Tillack, T W and Thompson, T E (1980) *Biochemistry* 19, 3919-3923
- 23 Wong, M, Anthony, F H, Tillack, T W and Thompson, T E (1980) *Biochemistry* 21, 4126-4132
- 24 Georghiou, S (1975) *Photochem Photobiol* 22, 103-109
- 25 Myers, M and Freire, E (1985) *Biochemistry* 24, 4076-4082
- 26 Batenburg, A M, Van Esch, J H and De Kruijff, B (1988) *Biochemistry* 27, 2324-2331
- 27 Dufourcq, J, Faucon, J-F, Fourche, G, Dasseux, J-L, Le Maire, M and Gulik-Krzywicki, T (1986) *Biochim Biophys Acta* 859, 33-48
- 28 Correa-Freire, M C, Freire, E, Barenholz, Y, Biltonen, R L and Thompson, T E (1979) *Biochemistry* 18, 442-445
- 29 Faucon, J-F and Lakowicz, J R (1987) *Arch Biochem Biophys* 252, 245-258
- 30 Vogel, H and Jähng, F (1985) *Proc Natl Acad Sci USA* 82, 2029-2033
- 31 Morgan, C G, Williamson, H, Fuller, S and Hudson, B (1983) *Biochim Biophys Acta* 732, 668-674
- 32 Eytan, G D and Almary, T (1983) *FEBS Lett* 156, 29-32
- 33 Bradrick, T D and Georghiou, S (1987) *Biochim Biophys Acta* 905, 494-498
- 34 Murata, M, Nagayama, K and Ohnishi, S-I (1987) *Biochemistry* 26, 4056-4062
- 35 Hong, K, Dizganes, N and Papahadjopoulos, D (1981) *J Biol Chem* 256, 3641-3644
- 36 Carner, C and Pérolet, M (1986) *Biochemistry* 25, 4167-4174
- 37 Dufourcq, E J, Faucon, J-F, Fourche, G, Dufourcq, J, Gulik-Krzywicki, T and Le Maire, M (1986) *FEBS Lett* 201, 205-209
- 38 Dawson, C R, Drake, A F, Helliwell, J and Hider, R C (1978) *Biochim Biophys Acta* 510, 75-86
- 39 Vogel, H, Jähng, F, Hoffman, V and Stumpel, J (1983) *Biochim Biophys Acta* 733, 201-209
- 40 Terwilliger, T C, Weissman, L and Eisenberg, D (1982) *Biophys J* 37, 353-361
- 41 Tosteson, M T and Tosteson, D C (1981) *Biophys J* 36, 109-116
- 42 Hanke, W, Methfessel, C, Wilmsen, H-U, Katz, E, Jung, G and Boehm, G (1985) *Biochim Biophys Acta* 727, 103-114
- 43 Terwilliger, T C and Eisenberg, D (1982) *J Biol Chem* 257, 6016-6022
- 44 Lis, L J, McAlister, M, Fuller, N, Rand, R P and Parsegian, V A (1982) *Biophys J* 37, 657-666
- 45 Mollay, C (1976) *FEBS Lett* 64, 65-68